

General Radial-Composition Correlations in Two-Component Many-Body Systems

Y. Lei (雷杨)*

School of Nuclear Science and Technology, Southwest University of Science and Technology, Mianyang 621010, China

(Dated: June 3, 2026)

The linear correlation between RMS radius difference and composition asymmetry in two-component many-body systems is a robust feature observed across nuclear experiments, diverse nuclear structural models, molecular dynamic simulations for bimetallic clusters, and galactic modeling with self-interacting dark matter. We identify the short-range attractive central force as the key ingredient for its emergence, a mechanism underpinned by the coordinate transformation under low-energy harmonic-oscillator approximation, the virial theorem, and Pauli principle/hard core potential, in many-fermion system/classic many-body system.

Complex bound many-body systems, such as nuclei, metallic nanoclusters, and galaxies, are central to understanding the universe and enabling practical applications [1]. Remarkably, although their interactions are complex and often not fully known, such systems exhibit striking regularities from a reductionist perspective. Examples include the nuclear $N_p N_n$ systematics [2], Wigner-Dyson level statistics in metallic clusters and quantum dots [3–6], and scaling relations for galaxy clusters and groups [7, 8]. The simplicity emerging from complexity often signals underlying dynamical and symmetry critical points, which merits deeper understanding.

For nuclear many-body system, random-interaction ensembles provide a unique and powerful framework for identifying robust patterns in nuclear systems [9–12]. By performing many-body calculations for pseudo nuclei with randomized interaction matrix elements, one can generate ensembles of resultant observables. Thus, features that emerge with statistical prevalence in such ensembles are considered independent of specific interaction details, such as the spin-zero and positive-parity ground states [13, 14], collective-like motions [15–20], and odd-even staggering in proton-neutron interactions [21]. Furthermore, specific sampling in random-interaction ensembles may reveal the key interaction features driving robust patterns, as Refs. [22–24].

Using this random-interaction approach[25], we study a general correlation between matter distribution and composition in two-component systems, from nuclei of protons and neutrons to galaxies of luminous and dark matter. We show that the difference between the root-mean-square (RMS) radii of the two components, $\Delta R = \sqrt{\langle r^2 \rangle_1} - \sqrt{\langle r^2 \rangle_2}$, is linearly correlated with the composition asymmetry, $I = (p_1 - p_2)/(p_1 + p_2)$, where $\sqrt{\langle r^2 \rangle_i}$ and p_i are the RMS radius and fraction of component i . Although this correlation has been observed in nuclear systems [26–32], it has remained unexplored in other systems. Here, we identify its key mechanism and employ various many-body methods to verify it at different scales. This scale-independent correlation may benefit future simulations, experiments, and observations of diverse many-body systems.

In nuclear physics, the quantity ΔR defined above is

known as the neutron skin thickness. It serves as the only laboratory proxy on earth, for neutron-matter stiffness and neutron-star radius [33–39]. Specifically, ΔR is found to be positively correlated with the symmetry energy slope L [40–42], a parameter that plays a decisive role in characterizing neutron star radii.

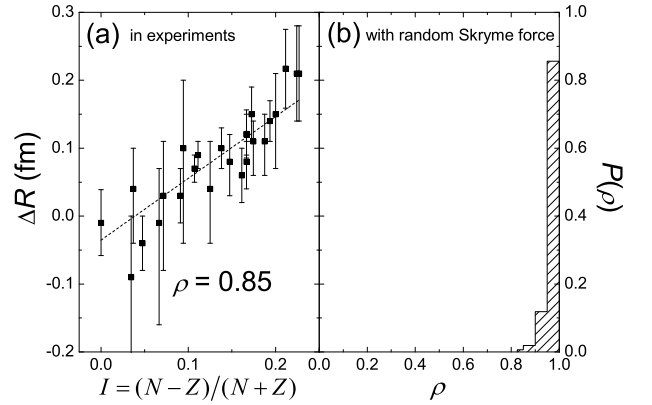


FIG. 1. Nuclear $\Delta R - I$ correlation. (a) Experimental data [43–47] give Pearson’s $\rho = 0.85$ [48]. (b) ρ distribution from random Skyrme-Hartree-Fock calculations [32]; the peak near $\rho \simeq 0.9$ shows robustness under random interactions.

Similarly, the quantity I defined above corresponds to the nuclear isospin asymmetry $(N - Z)/(N + Z)$. It has long been known that ΔR is positively correlated with I , as shown by experiments in Fig. 1(a). This linear trend is also robustly reproduced across diverse theoretical frameworks, e.g., liquid drop models, mean-field theories, and *ab initio* approaches [26–31]. We quantify this correlation with Pearson’s ρ [48]: $\rho = 1$ (0) for perfect (no) linearity. The experimental data yield $\rho = 0.85$, as shown in Fig. 1(a), confirming a robust linear trend. Remarkably, we recently noted that this correlation persists even under random parametrizations of the Skyrme force [32], as shown in Fig. 1(b). The robustness of this correlation across various theoretical calculations already suggests that this linearity may be largely independent of specific modeling details, and instead arises from few but intrinsic properties of the nuclear system.

To test the robustness of the $\Delta R - I$ correlation, we

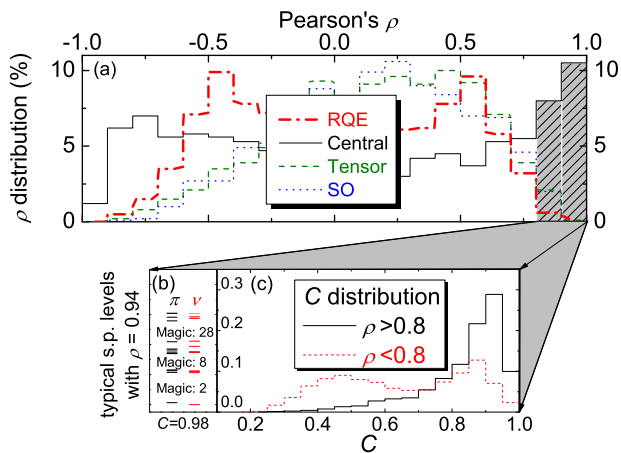


FIG. 2. (Color online) Nuclear $\Delta R - I$ correlation in random ensembles. (a) ρ Distribution for the $\Delta R - I$ correlation across different random ensembles: RQE, random central, tensor, and spin-orbit (SO) ensembles. The shaded region highlights the peak near $\rho = 0.9$ for the random central ensemble, from which data for (b) and (c) are taken. (b) Proton and neutron level schemes for a pseudo nucleus, ^{38}Ar , in a representative sample ($\rho = 0.94$), revealing clear gaps at harmonic oscillator (HO) magic numbers (2, 8, 28). The HO-likeness measure C for this pseudo ^{38}Ar , defined as the product of Pearson coefficients for proton and neutron spectra with exact 3D HO level scheme, equals to 0.98, suggesting a strong similarity of the spectra under investigation to HO ones. (c) C distributions for pseudo nuclei with $\rho > 0.8$ and $\rho < 0.8$ in the random central ensemble. Samples with $\rho > 0.8$ cluster at $C \simeq 0.9$, suggesting HO-like nature.

perform Hartree-Fock (HF) calculations [49–51] with several random ensembles. Calculation detail is described in Sec. I. We start with the random quasi-particle ensemble (RQE) [13], where two-body matrix elements are drawn randomly according to Eq. (1) of supp.pdf in the Supplemental Material [52], to maximize interaction freedom while preserving nuclear symmetries. For each RQE sample, Pearson's ρ is calculated with resultant ΔR and I of selected reference nuclei. Obtained ρ distribution appears in Fig. 2. The RQE yields a negligible probability (less than 1%) of strong correlation with $\rho > 0.9$, indicating that the $\Delta R - I$ linearity may not be guaranteed by nuclear symmetries but require specific physical drives in nucleon-nucleon interactions.

We test whether central, tensor, or spin-orbit forces drive the $\Delta R - I$ correlation, separately. These interaction types encompass all interactions that are independent of or linearly dependent on momentum, and compatible with general nuclear symmetries, specified by radial matrix elements of radial potential between nucleons [53]. We randomize these elements according to Eqs. (2), (4), and (6) of supp.pdf in the Supplemental Material [52], creating random central, tensor, and spin-orbit ensembles, respectively. The resulting ρ distributions are shown in Fig. 2. The random tensor and spin-orbit en-

sembles, like the RQE, fail to produce significant correlations with $P(\rho > 0.9) \approx 0$. In stark contrast, the random central ensemble exhibits a pronounced peak at $\rho \approx 0.95$, with nearly 20% of samples displaying strong linearity ($\rho > 0.8$). This statistical filtration unambiguously identifies the central force as the primary driver of the $\Delta R - I$ correlation.

Despite the central force being the primary driver, not all samples in the random central ensemble exhibit a strong $\Delta R - I$ correlation; additional features must distinguish those that do. To identify them, we select about 2000 samples with $\rho > 0.8$ from the 10000 in the ensemble and examine their HF single-particle spectra. Figure 2(b) shows a typical example for ^{38}Ar with $\rho = 0.94$, displaying clear shell closures at the harmonic-oscillator (HO) magic numbers (2, 8, 28) and nearly degenerate levels in the lowest two shells, resembling an HO spectrum. We quantify this HO-likeness by C , the product of Pearson coefficients between the proton (neutron) spectrum and the exact 3D HO spectrum; $C = 0.98$ for the example in Fig. 2(b). We then compute C for all samples with $\rho > 0.8$ and $\rho < 0.8$ shown in Fig. 2(c). The $\rho > 0.8$ samples, which roughly reproduce the $\Delta R - I$ correlation, are significantly more HO-like, with C peaked near 0.9, and vice versa. This suggests that an HO-like mean field underlies the nuclear $\Delta R - I$ correlation.

To directly examine the influence of the HO potential, we use a parameterized central-force HO potential $V^S(r) = V_0(r - r_0)^2$ for $S = 0, 1$, and apply it to the same reference nuclei as in the random central ensemble. We find that a repulsive HO force ($V_0 < 0$) consistently yields a roughly negative correlation ($\rho \approx -0.8$), contrary to nuclear observations. For attractive forces ($V_0 > 0$), the linearity is remarkably robust against the potential sharpness (V_0), yet sensitive to the potential minimum r_0 . Strong positive correlations ($\rho \approx 1$) only emerge when the minimum is localized within $r_0 < 1.5\sqrt{\hbar/m\omega}$; as r_0 increases, the correlation rapidly degrades to $\rho \approx -0.8$. We call a minimum near zero “short range”. Our results then show that the $\Delta R - I$ linearity is a hallmark of an attractive, short-range central HO interaction.

The emergence of the nuclear $\Delta R - I$ correlation from an attractive short-range HO potential may be supported by three pillars: the center-of-mass transformation, the virial theorem, and the Pauli principle. The center-of-mass transformation maps an HO interacting N -nucleon system to independent particles in a global HO mean field [54]. According to the virial theorem, in the HO mean field, the energy and potential, i.e., mean square radius, of HF single-particle states are proportional to each other. With the Pauli principle, nucleons sequentially occupy levels with increasing energy and, consequently, increasing spatial extent. The accumulation of like nucleons thus drives a systematic expansion of the total RMS radius. Thus, the asymmetry between proton and neutron numbers (I) is inherently correlated to their

RMS-radius difference (ΔR).

Realistic nuclear forces, though more complex than a zero-range HO, still induces the $\Delta R - I$ correlation [28–31]. That may be because this correlation come from nuclear ground states. In ground states, the low-energy minimum of any short-range potential can be approximated to a HO potential centered near $r = 0$, leading to the $\Delta R - I$ correlation. For example, random Skyrme forces [32], with dominant attractive zero-range central forces [55, 56], is expected to frequently yield this correlation as shown in Fig. 1(b). Thus, the key ingredient for the $\Delta R - I$ correlation in ground states of many-fermion system could be a short-range attractive central force.

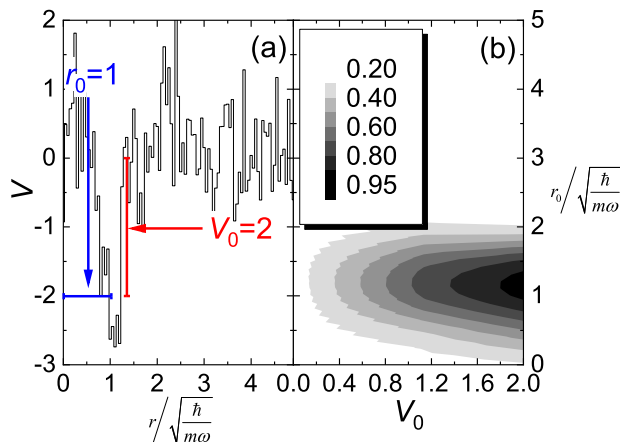


FIG. 3. (Color online) Random short-range ensemble. (a) Example potential ($S = 0$) at $V_0 = 2$, $r_0 = 1$, with V_0 (r_0) controlling degree of minimum attraction (minimum range). (b) $P(\rho > 0.9)$ as a function of V_0 and r_0 . The peak near ($V_0 = 2, r_0 = 1$) indicates that a short-range, attractive central force drives the $\Delta R - I$ correlation in nuclear ground states.

To test whether a short-range attractive central force produces the $\Delta R - I$ correlation in many-fermion systems, we construct “random short-range ensemble” with random spin-independent radial potentials, parameterized by degree of minimum attraction V_0 and minimum range r_0 according to Eq. (7) of supp.pdf in the Supplemental Material [52]. Fig. 3(a) shows a typical radial potential in such an ensemble. Random HF calculations yield $P(\rho > 0.9)$, the probability of $\rho > 0.9$, plotted against V_0 and r_0 in Fig. 3(b). The single peak at ($V_0 = 2, r_0 = 1$) confirms that a short-range attractive central force is essential for the $\Delta R - I$ correlation.

Although our discussion has been limited to nuclear quantum systems, the three pillars (coordinate transformation, virial theorem, and Pauli principle) supporting the explanation for the $\Delta R - I$ correlation may also apply classically. The first two pillars are valid for both quantum and classic systems. For the third one, in classical models of many-fermion systems, the Pauli principle can be mimicked by a hard core near $r = 0$. A hard core

forbids spatial overlap and converts particle number into spatial extent, much like the Pauli principle. Hence, a classical many-body system with short-range attraction and a hard core may also exhibit the $\Delta R - I$ correlation in low-energy states.

Molecular dynamics (MD) [57] simulation under Newton’s law for Cu_xAl_y nanoalloy clusters supports classic $\Delta R - I$ correlation and its mechanism. Taking such clusters as many-body systems, ΔR is the RMS radius difference between Cu and Al, and $I = (x - y)/(x + y)$ the composition asymmetry by atom count. We perform MD simulations with LAMMPS [58] to obtain the time-ergodic ground-state ΔR for nine reference CuAl clusters with different I , giving a Pearson’s ρ for each EAM potential. Calculation detail are described in Sec. II A 1 of supp.pdf in the Supplemental Material [52].

Alloy MD simulation usually adopts embedded-atom method (EAM) potential [59], where the pair potential carries most of the central force between atoms. Following random interaction approach, we randomize the pair potential to create simulation ensembles, to test the robustness of the $\Delta R - I$ correlation in a classical many-body system and to probe the role of short-range attraction. Based on the CuAl EAM potential [60] from the repository [61–63], we add Gaussian fluctuations to the attractive part as described by Eq. (8) of supp.pdf in the Supplemental Material [52] to generate a “random EAM” ensemble. A typical pair potential from this ensemble is shown in Fig. 4(a); it remains short-ranged and attractive.

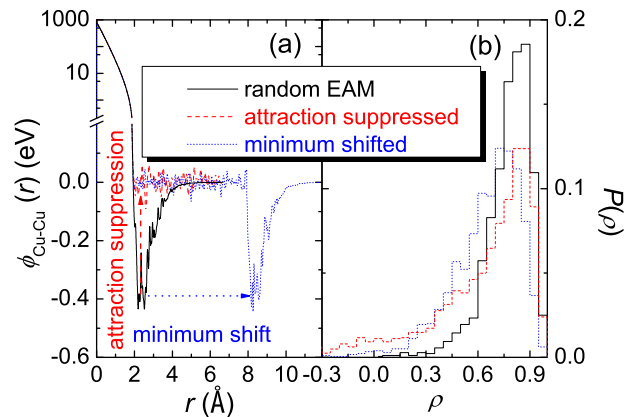


FIG. 4. (Color online) MD simulated CuAl clusters within random ensembles. (a) Typical Cu-Cu pair potentials from the random EAM, attraction-suppressed, and minimum-shifted ensembles. (b) Pearson’s ρ distributions for the three ensembles.

Random EAM ensemble frequently yields strong correlations with $P(\rho > 0.85) \approx 50\%$, and a peak near $\rho \approx 0.9$, as demonstrated by the resulting ρ distribution plotted in Fig. 4(b). To examine the correlation’s origin, we modify the pair potentials from Ref. [60] in two ways before randomization, yielding two ensembles. In

the “attraction-suppressed” ensemble the attractive part is set to zero. In the “minimum-shifted” ensemble the attractive part is shifted outward by 6 Å to create a long-range attraction, with the gap filled by zero. Both ensembles are then randomized as for random EAM ensemble. Figure 4(a) shows representative Cu-Cu potentials, and Fig. 4(b) gives their ρ distributions. Suppressing the attraction or making it long-range reduces $P(\rho > 0.85)$ by nearly 40% and shifts the peak of the distribution within minimum-shifted ensemble. These results confirm that, even in a classical many-body system, a short-range attractive central force is essential for the $\Delta R - I$ correlation.

The emergency mechanism of the $\Delta R - I$ correlation from a short-range attractive central force of classic many-body systems are supported by three pillars: coordinate transformations, the virial theorem, and a hard core between particles. To test this mechanism, one can remove one pillar and see if the correlation persists. Since the first two are generic, we focus on removing the hard core. This is difficult because a hard core ensures incompressibility of many-body system and prevents collapse into a singularity. For instance, in MD simulations of AlCu clusters, the EAM potential inherently supplies a strong repulsive core, and suppressing it will lead to numerical instabilities in LAMMPS [64]. Fortunately, in a two-component system one can remove the hard core for only one species, relying on the other to maintain global incompressibility. In a classical system, coreless particles with zero non-gravitational cross section must have nonzero mass to move under Newton’s laws, thus resembling weakly interacting massive particles, a dark matter candidate [65]. Then, we model the remaining component as “ordinary” matter undergoing elastic hard-ball collisions, characterized by a force range $r_o = 0.2$, while the dark matter particles interact only gravitationally, i.e., $r_d = 0$. Then gravity is introduced as a short-range central attraction acting on both species, constructing a minimal galactic model. Using the N -body integrator REBOUND [66, 67], we simulate this self-gravitating system, neglecting relativity, and compute Pearson’s ρ between ΔR , the difference between RMS radii of ordinary matter and dark matter, and the real-time composition asymmetry I for different initial I (details in Sec. II B of supp.pdf in the Supplemental Material [52]). As expected, for $r_d = 0$ ρ drifts away from 1 after initial fluctuation.

Figure 5 shows the time evolution of ρ for reference galaxies. For $r_d = 0$, ρ oscillates strongly before $t \sim 100$ and then decreases steadily, deviating from linearity after $t \sim 500$, as expected. Having shown that removing the hard core destroys the correlation, we now verify that restoring it recovers $\Delta R - I$. We assign a nonzero hard-ball force range r_d to dark matter, corresponding to strongly self-interacting dark matter recently proposed to address small-scale structure problems [68–70]. Dark

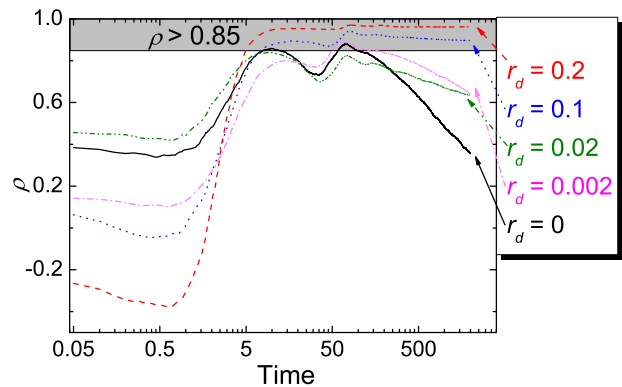


FIG. 5. (Color online) Time evolution of Pearson’s ρ for galaxy models with different initial composition asymmetry I and dark-matter hard-ball force range r_d . Time is shown on a log scale. The ordinary particles have $r_o = 0.2$. Five r_d values are considered: 0, 0.002, 0.02, 0.1, and 0.2.

matter and ordinary matter still interact only via gravity. When r_d is comparable to r_o ($r_d = 0.1$ or 0.2), the evolution stabilizes with $\rho > 0.85$, indicating that the correlation reappears. For $r_d = 0.02$, 0.002, or 0, no correlation emerges. Thus, hard-core potential for both components is required for the $\Delta R - I$ correlation emergency in classic systems, consistent with our understanding.

Furthermore, these results suggest that the $\Delta R - I$ correlation may serve as a fingerprint of dark-matter self-interactions. In our model, the correlation appears only when the dark-matter self-interaction cross section exceeds roughly 1% of the ordinary one. This could provide a novel upper limit on the dark-matter self-interaction cross section from galaxy surveys.

In summary, using random-interaction ensembles, we demonstrate and explain that the $\Delta R - I$ correlation in low-energy two-component fermionic and classical hard-core many-body systems is not a trivial consequence of many-body symmetries but stems from the short-range attraction of the central force, due to the coordinate transferability of the short-range HO-potential approximation and the virial theorem. In nuclear system, the robust appearance of the $\Delta R - I$ linearity across diverse theoretical frameworks [28–32] serves as a structural fingerprint of the short-range attraction of the nuclear force. Newtonian simulations of bimetallic clusters and galaxies with dark matter support this picture, indicating that the mechanism is neither scale nor quantum specific.

While our classical simulations produce the $\Delta R - I$ correlation, experimental verification on bimetallic clusters are still needed. This correlation may also probe dark matter self-interactions with more sophisticated simulations and observational galaxy surveys.

The author would like to acknowledge support by China Scholarship Council (Grant No. 202409390020).

- * leiyang1985@swust.edu.cn
- [1] B. Sherrill and R. F. Casten, Future articles: Frontiers of nuclear structure: Exotic nuclei, *Nuclear Physics News* **15**, 13 (2005), <https://doi.org/10.1080/10506890500454675>.
 - [2] R. F. Casten and N. V. Zamfir, The evolution of nuclear structure: the scheme and related correlations, *Journal of Physics G: Nuclear and Particle Physics* **22**, 1521 (1996).
 - [3] B. Wang, K. Wang, W. Lu, J. Yang, and J. G. Hou, Size-dependent tunneling differential conductance spectra of crystalline pd nanoparticles, *Phys. Rev. B* **70**, 205411 (2004).
 - [4] L. L. A. Adams, B. W. Lang, Y. Chen, and A. M. Goldman, Signatures of random matrix theory in the discrete energy spectra of subnanosize metallic clusters, *Phys. Rev. B* **75**, 205107 (2007).
 - [5] U. Sivan, R. Berkovits, Y. Aloni, O. Prus, A. Auerbach, and G. Ben-Yoseph, Mesoscopic fluctuations in the ground state energy of disordered quantum dots, *Phys. Rev. Lett.* **77**, 1123 (1996).
 - [6] S. R. Patel, S. M. Cronenwett, D. R. Stewart, A. G. Huibers, C. M. Marcus, C. I. Duruöz, J. S. Harris, K. Campman, and A. C. Gossard, Statistics of coulomb blockade peak spacings, *Phys. Rev. Lett.* **80**, 4522 (1998).
 - [7] N. Kaiser, Evolution and clustering of rich clusters, *Monthly Notices of the Royal Astronomical Society* **222**, 323 (1986), <https://academic.oup.com/mnras/article-pdf/222/2/323/1852806/mnras222-0323.pdf>.
 - [8] S. Giodini, L. Lovisari, E. Pointecouteau, S. Etori, T. H. Reiprich, and H. Hoekstra, Scaling relations for galaxy clusters: Properties and evolution, *Space Science Reviews* **177**, 247 (2013).
 - [9] V. Kota, Embedded random matrix ensembles for complexity and chaos in finite interacting particle systems, *Physics Reports* **347**, 223 (2001).
 - [10] Y. Zhao, A. Arima, and N. Yoshinaga, Regularities of many-body systems interacting by a two-body random ensemble, *Physics Reports* **400**, 1 (2004).
 - [11] V. Zelevinsky and A. Volya, Nuclear structure, random interactions and mesoscopic physics, *Physics Reports* **391**, 311 (2004), from atoms to nuclei to quarks and gluons: the omnipresent manybody theory.
 - [12] H. A. Weidenmüller and G. E. Mitchell, Random matrices and chaos in nuclear physics: Nuclear structure, *Rev. Mod. Phys.* **81**, 539 (2009).
 - [13] C. W. Johnson, G. F. Bertsch, and D. J. Dean, Orderly spectra from random interactions, *Phys. Rev. Lett.* **80**, 2749 (1998).
 - [14] Y. M. Zhao, A. Arima, N. Shimizu, K. Ogawa, N. Yoshinaga, and O. Scholten, Patterns of the ground states in the presence of random interactions: Nucleon systems, *Phys. Rev. C* **70**, 054322 (2004).
 - [15] R. Bijker and A. Frank, Band structure from random interactions, *Phys. Rev. Lett.* **84**, 420 (2000).
 - [16] Y. Lei, Z. Y. Xu, Y. M. Zhao, S. Pittel, and A. Arima, Emergence of generalized seniority in low-lying states with random interactions, *Phys. Rev. C* **83**, 024302 (2011).
 - [17] Y. Lu, Y. M. Zhao, N. Yoshida, and A. Arima, Correlations between low-lying yrast states for *sd* bosons with random interactions, *Phys. Rev. C* **90**, 064313 (2014).
 - [18] J. J. Shen, H. Jiang, and G. J. Fu, Robustness of “noncollective” rotational behavior for nuclei in the presence of random interactions, *Phys. Rev. C* **104**, 054319 (2021).
 - [19] C. White, A. Volya, D. Mulhall, and V. Zelevinsky, Structured ground states of randomly interacting bosons, *Phys. Rev. Res.* **5**, 013109 (2023).
 - [20] G. J. Fu and C. Qi, Novel triaxiality-driven collective feature in atomic nuclei investigated via the two-body random ensemble, *Phys. Rev. C* **112**, L061301 (2025).
 - [21] G. J. Fu, J. J. Shen, Y. M. Zhao, and A. Arima, Regularities in low-lying states of atomic nuclei with random interactions, *Phys. Rev. C* **91**, 054319 (2015).
 - [22] Y. Lei, Y. M. Zhao, N. Yoshida, and A. Arima, Correlations of excited states for *sd* bosons in the presence of random interactions, *Phys. Rev. C* **83**, 044302 (2011).
 - [23] Y. Lei, Robust correlations between quadrupole moments of low-lying 2^+ states within random-interaction ensembles, *Phys. Rev. C* **93**, 024319 (2016).
 - [24] Z.-Z. Qin and Y. Lei, Predominance of linear q and μ systematics in random-interaction ensembles, *Nuclear Science and Techniques* **29**, 163 (2018).
 - [25] Calculation details are all described in the supp.pdf of the Supplement Material [52].
 - [26] A. Trzcńska, J. Jastrzębski, P. Lubiński, F. J. Hartmann, R. Schmidt, T. von Egidy, and B. Klos, Neutron density distributions deduced from antiprotonic atoms, *Phys. Rev. Lett.* **87**, 082501 (2001).
 - [27] S. J. Novario, D. Lonardonì, S. Gandolfi, and G. Hagen, Trends of neutron skins and radii of mirror nuclei from first principles, *Phys. Rev. Lett.* **130**, 032501 (2023).
 - [28] W. D. Myers and W. Swiatecki, Average nuclear properties, *Annals of Physics* **55**, 395 (1969).
 - [29] W. Myers and W. Swiatecki, The nuclear droplet model for arbitrary shapes, *Annals of Physics* **84**, 186 (1974).
 - [30] W. Myers and W. Swiatecki, Droplet-model theory of the neutron skin, *Nuclear Physics A* **336**, 267 (1980).
 - [31] C. Pethick and D. Ravenhall, The dependence of neutron skin thickness and surface tension on neutron excess, *Nuclear Physics A* **606**, 173 (1996).
 - [32] Y. Lei, J. Qi, X. Lian, Z. Z. Qin, and C. L. Bai, Linear correlations related to neutron skin thickness, *Phys. Rev. C* **113**, 024314 (2026).
 - [33] B. Alex Brown, Neutron radii in nuclei and the neutron equation of state, *Phys. Rev. Lett.* **85**, 5296 (2000).
 - [34] C. J. Horowitz and J. Piekarewicz, Neutron star structure and the neutron radius of ^{208}pb , *Phys. Rev. Lett.* **86**, 5647 (2001).
 - [35] M. B. Tsang, J. R. Stone, F. Camera, P. Danielewicz, S. Gandolfi, K. Hebeler, C. J. Horowitz, J. Lee, W. G. Lynch, Z. Kohley, R. Lemmon, P. Möller, T. Murakami, S. Riordan, X. Roca-Maza, F. Sammarruca, A. W. Steiner, I. Vidaña, and S. J. Yennello, Constraints on the symmetry energy and neutron skins from experiments and theory, *Phys. Rev. C* **86**, 015803 (2012).
 - [36] G. Hagen, A. Ekström, C. Forssén, G. R. Jansen, W. Nazarewicz, T. Papenbrock, K. A. Wendt, S. Bacca, N. Barnea, B. Carlsson, C. Drischler, K. Hebeler, M. Hjorth-Jensen, M. Miorelli, G. Orlandini, A. Schwenk, and J. Simonis, Neutron and weak-charge distributions of the ^{48}Ca nucleus, *Nature Physics* **12**, 186 (2016).
 - [37] B. A. Brown, Mirror charge radii and the neutron equation of state, *Phys. Rev. Lett.* **119**, 122502 (2017).
 - [38] F. J. Fattoyev, J. Piekarewicz, and C. J. Horowitz, Neutron skins and neutron stars in the multimessenger era,

- Phys. Rev. Lett.* **120**, 172702 (2018).
- [39] C. A. Bertulani and J. Valencia, Neutron skins as laboratory constraints on properties of neutron stars and on what we can learn from heavy ion fragmentation reactions, *Phys. Rev. C* **100**, 015802 (2019).
- [40] X. Roca-Maza, M. Centelles, X. Viñas, and M. Warda, Neutron skin of ^{208}Pb , nuclear symmetry energy, and the parity radius experiment, *Phys. Rev. Lett.* **106**, 252501 (2011).
- [41] P.-G. Reinhard and W. Nazarewicz, Nuclear charge and neutron radii and nuclear matter: Trend analysis in skyrme density-functional-theory approach, *Phys. Rev. C* **93**, 051303 (2016).
- [42] A. Steiner, M. Prakash, J. Lattimer, and P. Ellis, Isospin asymmetry in nuclei and neutron stars, *Physics Reports* **411**, 325 (2005).
- [43] J. Zenihiro, H. Sakaguchi, S. Terashima, T. Uesaka, G. Hagen, M. Itoh, T. Murakami, Y. Nakatsugawa, T. Ohnishi, H. Sagawa, H. Takeda, M. Uchida, H. P. Yoshida, S. Yoshida, and M. Yosoi, *Direct determination of the neutron skin thicknesses in $^{40,48}\text{Ca}$ from proton elastic scattering at $e_p = 295$ mev* (2018), arXiv:1810.11796 [nucl-ex].
- [44] J. JASTRZEBSKI, A. TRZCIŃSKA, P. LUBIŃSKI, B. KŁOS, F. J. HARTMANN, T. von EGIDY, and S. WYCECH, Neutron density distributions from antiprotonic atoms compared with hadron scattering data, *International Journal of Modern Physics E* **13**, 343 (2004), <https://doi.org/10.1142/S0218301304002168>.
- [45] W. R. Gibbs and J.-P. Dedonder, Neutron radii of the calcium isotopes, *Phys. Rev. C* **46**, 1825 (1992).
- [46] D. Adhikari, H. Albataineh, D. Androic, K. A. Aniol, D. S. Armstrong, T. Averett, C. Ayerbe Gayoso, S. K. Barcus, V. Bellini, R. S. Beminiwattha, J. F. Benesch, H. Bhatt, D. Bhatta Pathak, D. Bhetuwal, B. Blaikie, J. Boyd, Q. Campagna, A. Camsonne, G. D. Cates, Y. Chen, C. Clarke, J. C. Cornejo, S. Covrig Dusa, M. M. Dalton, P. Datta, A. Deshpande, D. Dutta, C. Feldman, E. Fuchey, C. Gal, D. Gaskell, T. Gautam, M. Gericke, C. Ghosh, I. Halilovic, J.-O. Hansen, O. Hassan, F. Hauenstein, W. Henry, C. J. Horowitz, C. Jantzi, S. Jian, S. Johnston, D. C. Jones, S. Kakkar, S. Katugampola, C. Keppel, P. M. King, D. E. King, K. S. Kumar, T. Kutz, N. Lashley-Colthirst, G. Leverick, H. Liu, N. Liyanage, J. Mammei, R. Mammei, M. McCaughan, D. McNulty, D. Meekins, C. Metts, R. Michaels, M. Mihovilovic, M. M. Mondal, J. Napolitano, A. Narayan, D. Nikolaev, V. Owen, C. Palatchi, J. Pan, B. Pandey, S. Park, K. D. Paschke, M. Petrusky, M. L. Pitt, S. Premathilake, B. Quinn, R. Radloff, S. Rahman, M. N. H. Rashad, A. Rathnayake, B. T. Reed, P. E. Reimer, R. Richards, S. Riordan, Y. R. Roblin, S. Seeds, A. Shahinyan, P. Souder, M. Thiel, Y. Tian, G. M. Urciuoli, E. W. Wertz, B. Wojtsekhowski, B. Yale, T. Ye, A. Yoon, W. Xiong, A. Zec, W. Zhang, J. Zhang, and X. Zheng (CREX Collaboration), Precision determination of the neutral weak form factor of ^{48}Ca , *Phys. Rev. Lett.* **129**, 042501 (2022).
- [47] G. Giacalone, G. Nijs, and W. van der Schee, Determination of the neutron skin of ^{208}Pb from ultrarelativistic nuclear collisions, *Phys. Rev. Lett.* **131**, 202302 (2023).
- [48] P. Karl, VII. note on regression and inheritance in the case of two parents, *Proc. R. Soc. Lond.* **58**, 240 (1895).
- [49] I. Stetcu and C. W. Johnson, Random phase approximation vs exact shell-model correlation energies, *Phys. Rev. C* **66**, 034301 (2002).
- [50] I. Stetcu and C. W. Johnson, Tests of the random phase approximation for transition strengths, *Phys. Rev. C* **67**, 044315 (2003).
- [51] I. Stetcu and C. W. Johnson, Gamow-teller transitions and deformation in the proton-neutron random phase approximation, *Phys. Rev. C* **69**, 024311 (2004).
- [52] See Supplemental Material at URL will be inserted by publisher.
- [53] R. Lawson, *Theory of the Nuclear Shell Model*, Oxford studies in nuclear physics (Clarendon Press, 1980).
- [54] J. P. Elliott and T. H. R. Skyrme, Centre-of-mass effects in the nuclear shell-model, *Proceedings of the Royal Society of London. A. Mathematical and Physical Sciences* **232**, 561 (1955), <https://royalsocietypublishing.org/rspa/article-pdf/232/1191/561/49>
- [55] T. H. R. Skyrme, A non-linear field theory, *Proceedings of the Royal Society of London. A. Mathematical and Physical Sciences* **260**, 127 (1961), <https://royalsocietypublishing.org/rspa/article-pdf/260/1300/127/52>
- [56] T. Skyrme, The effective nuclear potential, *Nuclear Physics* **9**, 615 (1958).
- [57] P. Tian, Molecular dynamics simulations of nanoparticles, *Annu. Rep. Prog. Chem., Sect. C: Phys. Chem.* **104**, 142 (2008).
- [58] A. P. Thompson, H. M. Aktulga, R. Berger, D. S. Bolinteanu, W. M. Brown, P. S. Crozier, P. J. in 't Veld, A. Kohlmeyer, S. G. Moore, T. D. Nguyen, R. Shan, M. J. Stevens, J. Tranchida, C. Trott, and S. J. Plimpton, LAMMPS - a flexible simulation tool for particle-based materials modeling at the atomic, meso, and continuum scales, *Comp. Phys. Comm.* **271**, 108171 (2022).
- [59] S.-G. Kim, M. F. Horstemeyer, M. I. Baskes, M. Rais-Rohani, S. Kim, B. Jelinek, J. Houze, A. Moitra, and L. Liyanage, Semi-empirical potential methods for atomistic simulations of metals and their construction procedures, *Journal of Engineering Materials and Technology* **131**, 041210 (2009), <https://asmedigitalcollection.asme.org/materialstechnology/article-p>
- [60] J. Cai and Y. Y. Ye, Simple analytical embedded-atom-potential model including a long-range force for fcc metals and their alloys, *Phys. Rev. B* **54**, 8398 (1996).
- [61] L. M. Hale, Z. T. Trautt, and C. A. Becker, Evaluating variability with atomistic simulations: the effect of potential and calculation methodology on the modeling of lattice and elastic constants, *Modelling and Simulation in Materials Science and Engineering* **26**, 055003 (2018).
- [62] C. A. Becker, F. Tavazza, Z. T. Trautt, and R. A. Buarque de Macedo, Considerations for choosing and using force fields and interatomic potentials in materials science and engineering, *Current Opinion in Solid State and Materials Science* **17**, 277 (2013), *frontiers in Methods for Materials Simulations*.
- [63] C. A. Becker, F. Tavazza, Z. T. Trautt, and R. A. Buarque de Macedo, *Interatomic Potentials Repository*, <https://www.ctcms.nist.gov/potentials> (2013), national Institute of Standards and Technology (NIST).
- [64] T. C. Beutler, A. E. Mark, R. C. van Schaik, P. R. Gerber, and W. F. van Gunsteren, Avoiding singularities and numerical instabilities in free energy calculations based on molecular simulations, *Chemical Physics Letters* **222**, 529 (1994).

- [65] L. Roszkowski, E. M. Sessolo, and S. Trojanowski, Wimp dark matter candidates and searches-current status and future prospects, *Reports on Progress in Physics* **81**, 066201 (2018).
- [66] Rein, H. and Liu, S.-F., Rebound: an open-source multi-purpose n -body code for collisional dynamics, *A&A* **537**, A128 (2012).
- [67] H. Rein and D. S. Spiegel, ias15: a fast, adaptive, high-order integrator for gravitational dynamics, accurate to machine precision over a billion orbits, *Monthly Notices of the Royal Astronomical Society* **446**, 1424 (2015), <https://academic.oup.com/mnras/article-pdf/446/2/1424/9381126/stu2164.pdf>.
- [68] Y. Hochberg, E. Kuflik, T. Volansky, and J. G. Wacker, Mechanism for thermal relic dark matter of strongly interacting massive particles, *Phys. Rev. Lett.* **113**, 171301 (2014).
- [69] J. Smirnov and J. F. Beacom, New freezeout mechanism for strongly interacting dark matter, *Phys. Rev. Lett.* **125**, 131301 (2020).
- [70] Y.-D. Tsai, R. McGehee, and H. Murayama, Resonant self-interacting dark matter from dark qcd, *Phys. Rev. Lett.* **128**, 172001 (2022).